Insights gained using HHMS-PI from the Sun to Voyager 2

Devrie S. Intriligator, Thomas Detman, Murray Dryer, James Intriligator, Wei Sun, William R. Webber, and Charles Deehr

Citation: AIP Conference Proceedings **1436**, 314 (2012); doi: 10.1063/1.4723625
View online: http://dx.doi.org/10.1063/1.4723625
View Table of Contents: http://scitation.aip.org/content/aip/proceeding/aipcp/1436?ver=pdfcov
Published by the AIP Publishing

Insights Gained using HHMS-PI from the Sun to Voyager 2

Devrie S. Intriligator [1], Thomas Detman[1], Murray Dryer [1],

James Intriligator [1,2], Wei Sun[1,3], William R. Webber[4], and Charles Deehr[1,3]

1. Carmel Research Center, P.O. Box 1732, Santa Monica, CA 90406, USA
2. Bangor University, Bangor, Wales, LL572AS, UK
3. Geophysical Institute, University of Alaska, Fairbanks, AK 99775, USA
4. New Mexico State University, Las Cruces, NM 88005, USA

Abstract. We extended the three-dimensional (3D) time-dependent magnetohydrodynamic (MHD) Hybrid Heliospheric Modeling System with Pickup Protons (HHMS-PI) [1] out to Voyager 2 (V2) and to 75 AU. HHMS-PI starts at the Sun and uses pre- and post- event background mode source surface (SS) solar inputs and solar event inputs. Our scientific results include good agreement between the HHMS-PI simulated parameters of the solar wind (SW) and interplanetary magnetic field (IMF) measurements at ACE, Ulysses, and Cassini. HHMS-PI simulates well the strong shocks observed at ACE, Ulysses, and Cassini associated with the Halloween 2003 solar events. This agreement indicates that HHMS-PI can provide good simulations for the Sedov strong shock limit. Comparisons between HHMS-PI simulated shock propagation from the Sun to Ulysses and Cassini and the spacecraft measurements of shock arrivals indicates that pickup protons slow the propagation of shocks to Ulysses and Cassini. Our simulations also demonstrate the importance of asymmetric flows in latitude and in longitude. For the Halloween 2003 solar events the HHMS-PI simulations show the large extent in latitude and in longitude of the shocks. The HHMS-PI simulations also indicate that IMF sector boundaries are greatly affected by the SW/IMF.
Keywords: solar variability effects, solar wind plasma & fields, interplanetary magnetic fields, interplanetary propagation, heliosphere interstellar medium interaction, shocks, pickup ions
PACS: 96.60.Q.-, 96.50sh, 96.50-e, 96.50.Bh, 96.50Xy,96.50Ya,96.60

INTRODUCTION

There is a great deal of interest in the SW and IMF parameters, pickup proton parameters, heliospheric variability, and asymmetries throughout the heliosphere. Now that both Voyager 1 (V1) and 2 (V2) have been crossed by the termination shock (TS), there is evidence [2] of the apparent asymmetry in the TS location between the north and south heliospheric hemispheres: V1 at 34° North was crossed in 2004 by the TS at 94 AU, and V2 at 27° South was crossed in 2007 by the TS near 84 AU. While some of this asymmetry may be due to the north/south asymmetry in the heliosphere caused by the magnitude and direction of the Local Interstellar Medium (LISM) magnetic field [3], some of it may be due to temporal changes in the heliosphere associated with solar cycle changes on the Sun [2]. IBEX integrated line of sight observations [4] revealed an Energetic Neutral Atom (ENA) ribbon in the LISM that also may be affected by the properties of the LISM, asymmetries, and the locations of the TS and the Heliopause (HP), as well as by heliospheric variability due to solar activity.

Detman et al. (2011) [1] summarized the physics of HHMS-PI and detailed many of its simulation results for the Halloween 2003 solar events [5] at ACE and Ulysses. HHMS-PI [1] starts at the Sun, the origin of the SW and IMF, and is a 3D MHD time-dependent modeling system that also specifically includes the effects of pickup protons, and simulates both the slowly evolving background and disturbed SW and IMF throughout the 3D heliosphere. Figure 1, adapted from [1], shows the schematic of HHMS-PI. The left side of the schematic shows how the background SW is simulated using source surface maps that supply information on coronal

Physics of the Heliosphere: A 10 Year Retrospective
AIP Conf. Proc. 1436, 314-320 (2012); doi: 10.1063/1.4723625

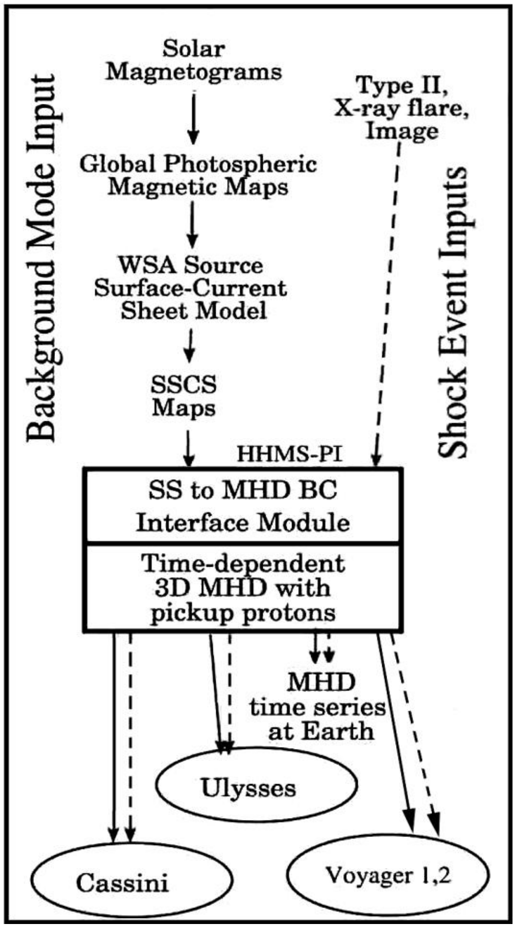

Fig.1. Diagram of HHMS-PI from the Sun to V1&V2. Left side/solid arrows: background mode. Right side/dashed arrows: event mode.

holes, magnetic fields, and other long-lived solar features. The right side of Fig. 1 illustrates the HHMS-PI solar event simulation using localized perturbations of the model's boundary conditions (BC's). These perturbations are based on observations of Type II radio bursts, flares, coronal mass ejections (CMEs), and other transient solar features.

Our approach is the only one that uses 3D models driven *continuously* by solar data. It is the only approach that accurately describes and analyzes the IMF structures (shocks, corotating interaction regions, stream-stream interactions) that can lead to strong heliospheric effects. At present our team is the only one with such models. Under our current NASA grant we have improved our models, including the effects of pickup protons in HHMS-PI, and running it out to 75 AU for more than eleven solar rotations. Our past work [5-9] using these models showed that significant global heliospheric asymmetries often evolve over time. While in-situ data (e.g., at L1) are valuable (e.g., they help to refine or "tune" a model), any model (1D, 2D, or even 3D) that relies only on such data as inputs can often make erroneous predictions because shock-induced effects can miss entirely a given location. Also, any attempt to model the propagation of solar phenomena must begin at their source – the Sun. Such propagation is dependent on the state of the medium through which it is propagating, so models must incorporate these continuously varying pre- and post-event states. The unsteady and highly non-linear 3D nature of heliospheric conditions and propagating disturbances requires the use of 3D time-dependent global models such as ours. We examine in our models, within acceptably measured limits and through careful tuning procedures, the accuracy/possible uncertainties that are endemic to all 3D MHD and other models.

The flow of information in HHMS-PI begins with ~ daily solar magnetograms that are combined into global solar magnetic maps. Those are input to the Wang-Sheeley-Arge (WSA) Source Surface (SS) Current Sheet Model [9]. The output of the WSA model is a set of source surface maps (at a height of 5 solar radii (R_S) of radial magnetic field, and various topological parameters of the magnetic field in the solar corona, between the photosphere and 5 R_S. HHMS-PI contains an empirical interface model (or module) that translates source surface map parameters into MHD boundary conditions to drive the SW model. This is the background mode on the left side of Fig. 1. The empirical interface contains adjustable parameters that we "tune" to maximize the "skill" (as described below) of the simulated SW using ACE data as the reference. Generally, we tune the model using a quiet interval preceding the events we wish to study.

If taken out of context, our use of a SS model, an empirical interface, and its tuning, could be criticized. However, our interest is not in the corona. Our interest is in the dynamic solar wind, especially in the outer heliosphere (OH); in studying the impact of solar activity, especially disturbances; in the OH; and in the role played by pickup protons in these areas. Having good (correct) solar wind BC's is essential. Our approach gives us that. Coronal modeling is a challenging research area in its self, but we leave it to others and watch for results we can use.

Our approach is to use 3D time-dependent numerical SW models driven continuously by solar data and to tune our models and model inputs using spacecraft (s/c) data to reconstruct the dynamic SW response to selected periods of solar activity. More details of our models, including the pickup proton model, are described in [1]. We look for and test ways to improve our models, our model inputs, and our results. We do this objectively and quantitatively by using rigorous verification of our simulations against the s/c data ("benchmarking") that they are intended to reproduce. For the purpose of tuning model parameters and shock inputs, we use a standard forecast verification metric: "skill" [1]. We compute skills for a set of simulated solar wind parameters versus the corresponding s/c observations, we do this for each s/c used in the run, then we average all the skills into one number: a skill for the run. This allows us to rank each run, and to assess improvements objectively.

We define [1] the skill, also known as Prediction Efficiency, as: PE=1–MSE/VAR where MSE is the mean squared error and VAR is the variance of the observed time series. We also give the more familiar standard correlation coefficients (rc's) between simulated and observed variables.

HHMS-PI AND SPACECRAFT MEASUREMENT COMPARISONS

Figure 2 shows for the Halloween 2003 solar events a comparison between the HHMS-PI ACE simulation and ACE measurements. At this time ACE was located at Heliographic Inertial Coordinate (HGI) latitude of 4° and longitude 327°. The relatively good skill scores and correlation coefficients indicate good agreement between this 3D MHD time-dependent HHMS-PI simulation and the ACE data. The ACE data are in blue, the HHMS-PI simulations are in red. The purple line in the top panel shows the HHMS-PI boundary condition (BC) input speed at 21 R_S (0.1 AU). Shock perturbations are apparent. In the first phase of HHMS-PI simulations, only one event input parameter, the shock speed (i.e., its departure speed from the Sun) for each event, was tuned [1] to the ACE data. The second phase considered shock arrivals at both ACE and Ulysses. During the second phase [1], two (and sometimes three) shock input parameters associated with solar events (the right side of Fig. 1) were adjusted (tuned): (a) the location of the event on the Sun; (b) its departure speed from the Sun, and, sometimes (c) the duration of the event input pulse at the Sun. An interesting outcome of this "bi-tuning" of shock inputs to match shock arrivals at both ACE and Ulysses was the necessary addition of another event to represent a CME on the backside of the Sun whose effects were observed in the Ulysses data [1,9]. HHMS-PI with these adjusted (tuned) solar inputs was run again in 3D from the Sun to ACE, Ulysses, Cassini, and V2.

Some criticism has come to our attention about the ability of our basic MHD model [11,12] to replicate the classical theory of Sedov [13] for strong shocks. However, this criticism is incorrect since our MHD model solves the MHD equations in conservation form [1]; it is thus a "shock capturing" code. Sedov theory uses a similarity transformation from partial to ordinary differential equations (gas dynamics). For the limiting strong shock (Rankine-Hugoniot) density jump, the theory gives $N_2/N_1=(\gamma+1)/(\gamma-1)$. In the case of the Halloween 2003 strong shock at ACE, this criticism was shown to be invalid when the HHMS-PI code [1] simulated (for $\gamma = 5/3$)

the density jump of 4.13 for the 28 October 2003 (DOY 301) shock at ACE from the X17.2 flare and CME at E08 earlier on the same day (see Fig. 2). Furthermore, we routinely use the jump in entropy produced by shock energy dissipation as a means of tracking shock locations in our model's grid (see Fig. 3 and text).

The good agreement shown in the SW speed and other parameters for the two strong shocks between Days 300 to 310, 2003 at ACE (Fig. 1) are convincing evidence that HHMS-PI can provide reliable simulations associated with strong shocks in the limiting Sedov solution. There also is good agreement (not shown) between the HHMS-PI simulations and the Ulysses [1] and Cassini [14] measurements for the arrival times of the shocks, the changes in speed magnitudes, and the duration of the disturbances in the SW and IMF parameters associated with the events.

Figure 3 is a radius-time (RT) plot from the Sun to 10 AU along the Sun-Saturn (Cassini) line of an entropy-based shock index [1]. The index is d/dr (log (P/ρ^{γ})) where P denotes the thermal pressure, ρ the mass density, and γ the polytropic index. In Fig. 3 forward shocks (FSs), and reverse shocks (RSs), are seen as blue lines, and red lines respectively, and sector boundaries (SBs) are denoted by dotted lines. The multiple shock interactions shown, just beyond 1 AU, are in close agreement with the kinematic model results [5-8]. This point is an extremely important qualitative difference from other existing 3D MHD models in the following sense: the HAFSS [5-8] kinematic model has been extensively tested in real time, and the HHMS-PI MHD model has confirmed these results in ex post facto studies as shown by the shock tracks in Fig. 3. Fig. 3 shows the Halloween 2003 shock trajectories that were obtained at one stage in our benchmarking process. Shock inputs were tuned to match shock times of arrivals (ToA's) at both ACE and Ulysses; then we went to 10 AU and compared results with Cassini data. Then we expanded the model again, and tracked these events to V2. In Fig. 3 the circles, at Cassini, are observed ToA's [1,14] and the +'s are HHMS-PI simulated ToA's. These diagnostic plots greatly assist the analysis of SW/IMF configurations. In [14] the specific effect of pickup protons on shock propagation are quantified by comparing two HHMS-PI runs to 10 AU which were identical except that one had the neutral H distribution described in [1], and the other had the neutral H density set to zero. The result was that the presence of pickup protons, from neutral H, caused all of the shocks reaching Cassini (Fig. 3) to be delayed. The average delay was 26.7 hours. For the same two runs, all shock arrivals at Ulysses were delayed for the case with pickup protons, the average being 17.6 hours [1]. At ACE we found no differences in the shock arrival times. These results are consistent with our expectations. We expect that as HHMS-PI pickup proton modeling improves, such agreements will increase between the observed/modeled shock arrivals. The analysis, based on Fig. 3, is fruitful since it shows for the first time the effects pickup protons can have on shock propagation [1,14]. We plan to continue using this benchmarking methodology.

Figures 4 to 6 show some results from a recent run that was a first test of three HHMS-PI "improvements": a new BC interface module, the addition of heat flux close to the Sun, and dropping the use of γ as the polytropic index by restoring it to the ratio of specific heats, 5/3, for adiabatic flow. We extended the HHMS-PI grid to 75 AU to include V2 at 73 AU. The addition of heat flux close to the Sun altered shock formation, as expected. Thus our tuned shock inputs were somewhat de-tuned by this model change. However, reasonably good results were obtained for both background and shocks at ACE, Ulysses, and Cassini. But at V2, the test run gave speeds and temperatures much lower than those observed at V2, and thus reduced shock speeds.

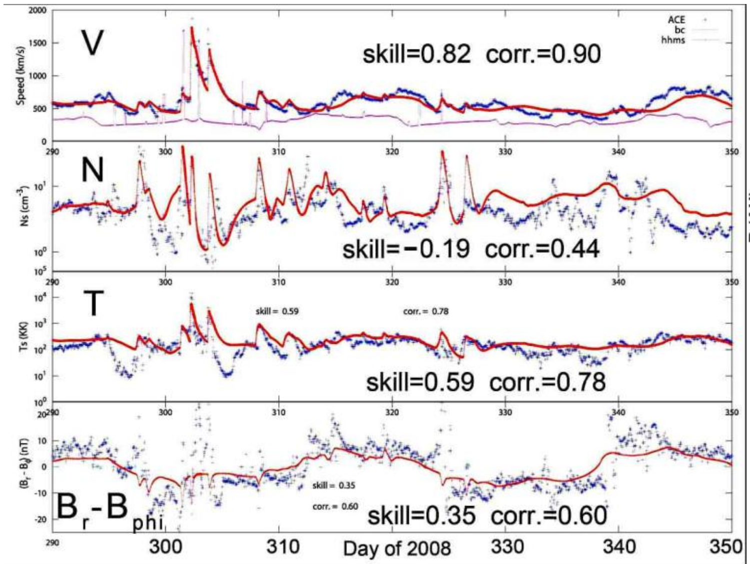

Fig. 2. HHMS-PI (red), ACE (blue) – V, N, T, & (Br-Bφ); and BC (purple) for Halloween 2003. Note good skill and rc scores for V.

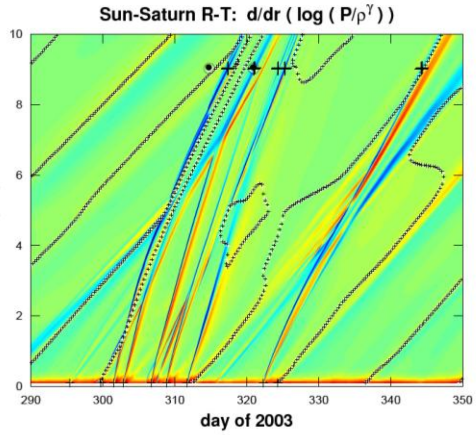

Fig. 3. HHMS-PI Sun-Saturn radius-time plot of entropy-based shock index, from new 75 AU test run. Blue – Forward shocks. Red – Reverse shocks. Dotted lines – IMF sector boundaries. Circles are observed ToA's at Cassini; crosses are HHMS-PI simulated ToA's.

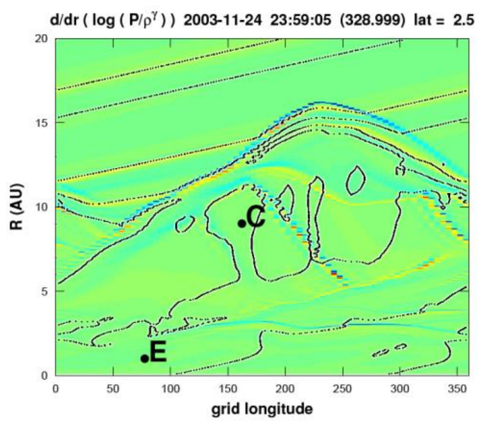

Fig. 4. Latitude 2.5° N slice through grid showing entropy-based shock index out to 20 AU on 2003-11-24. Fwd. shocks - blue. Rev. shocks - red. Dotted lines are sector boundaries. Note large distortions.

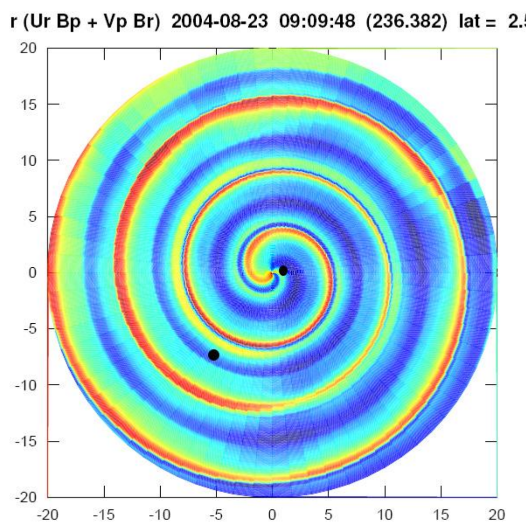

Fig. 5. Latitude 2.5°N slice through grid showing MHD flow invariant related to IMF polarity; red - away; blue - toward. Dots mark location of Earth and Saturn (Cassini).

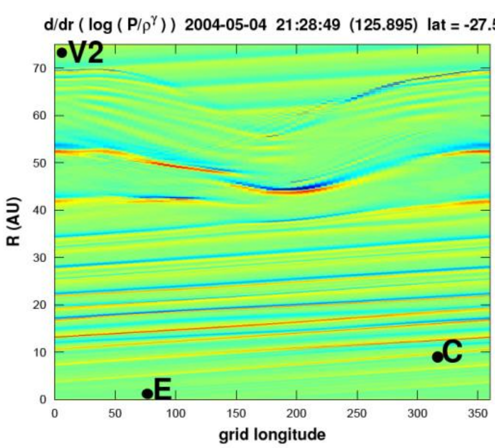

Fig. 6. (To left) Latitude - 27.5°S (near V2) grid slice showing entropy-based shock index to 75 AU (full grid) on 2004-05-04. Forward shocks - dark blue. Reverse shocks - red. Dots mark Earth, Saturn (Cassini), and V2 (upper left) locations. Note large extent of shock deformations & asymmetries at R > 40 AU.

We have gone back to the previous model, no heat flux, and γ =1.5. It is running now to 75 AU.

Figure 4 is a radius-longitude plot to 20 AU of the same entropy-based shock index that is shown in Fig. 3. Figure 4 shows a slice through a HHMS-PI grid at 2.5°N. It displays our entropy-based shock index, from our first test run, out to 20 AU. The locations of Earth and Saturn, in the model grid, are marked by black dots. Note! The longitude on the horizontal axis is that of the model's grid, it should not be confused with any standard coordinate system. (Currently, the model grid rotates once per year so that Earth stays at a fixed longitude in the model grid.) We plan to modify the model to eliminate this historical legacy, and make HHMS-PI operate in other coordinates (e.g., ecliptic, HGI). The intersection of the HCS with the latitude 2.5°N conical section is marked by tiny alternating back and white dots. Note the large distortion of the HCS due to the large shocks propagating outward. Fig. 4 emphasizes the distortions of the sector boundaries, which are tangential discontinuities (TDs) that balance the total of the SW and IMF pressures on each side of the TD. Note the large extent of the shock in AU and degrees, e.g., the large distortion near 10 AU which extends from about 50 degrees to beyond 300 degrees.

Figure 5 is a HHMS-PI polar plot from the Sun to 20 AU of the MHD flow invariant [1]: R (Ur Bφ + Vφ Br) that is related to the IMF polarity, "away" polarity is yellow to red, and "toward" polarity is cyan to blue. Fig. 5 shows this pinwheel plot well after the Halloween 2003 events are gone and the model grid has returned to a normal, quiet time spiral pattern. The spiral configuration of the IMF is evident in Fig. 5.

Figure 6 (similar to Fig. 4) shows the entropy based shock index for the full radial extent of the grid, 75 AU, at latitude -27.5° from our first test run using the revised BC's, etc. as discussed above. At the time of this plot, -27.5° is the closest grid latitude to the V2 spacecraft. The small black dot in the top left corner marks the location of V2 in the model grid. (Plot longitudes refer only to model grid.) Note the large extent (in AU & degrees) of the shocks. Notice the inner part of the grid (< ~ 30 AU) has returned to quiet, slowly evolving, background conditions.

SUMMARY

We extended the 3D time-dependent MHD model HHMS-PI [1] out to 75 AU and to V2 (73 AU). We simulated quiet and active (shock) periods, including the Halloween 2003 solar events. The HHMS-PI simulations show that pickup protons slow the propagation of the solar wind and shocks. Other HHMS-PI scientific results include evidence of large-scale asymmetric solar wind flows in latitude and longitude, and good agreement with ACE, Ulysses, and Cassini solar wind and IMF data. Sector boundaries are greatly affected by SW/IMF pressure changes. We believe that our methodology of "bi-tuning" continuous, and often, multiple solar events *starting at the Sun* is essential for a physically realistic simulation of the outer heliosphere. Hence alternative individual and single event modeling that avoids this realistic scenario are inappropriate. We look forward to extending the capabilities of HHMS-PI and to examining other quiescent and disturbed times in the solar wind from the Sun to V2 and V1 in the outer heliosphere.

ACKNOWLEDGMENTS

The work at Carmel Research Center was supported in part by NASA grant NNX08AE40G and by Carmel Research Center, Inc.

REFERENCES

1. T. R. Detman, D. S. Intriligator, M. Dryer, W. Sun, C. S. Deehr, and James Intriligator, The influence of pickup protons, from interstellar neutral hydrogen, on the propagation of the interplanetary shocks to ACE and Ulysses from the Halloween 2003 solar events: A 3D MHD modeling study, *J. Geophys. Res.*, *116*, A06105, doi: 10.1029/2010JA015803, 2011.
2. W. R. Webber and D. S. Intriligator, Voyagers 1 and 2 in a shrunken and squashed heliosphere, *J. Geophys. Res*., 116, A07107, doi: 10.1029/2011JA016478, 2011.
3. R. Lallement, E. Quemerais, J. L. Bertaux,et al., Deflection of the Interstellar Neutral Hydrogen Flow Across the Heliospheric Interface, *Science*, 307, 1447, 2005.
4. D. McComas et al., Global Observations of the Interaction from the Interstellar Boundary Explorer (IBEX), *Science*, 326, 959, 2009.
5. D. S. Intriligator, W. Sun, M. Dryer, C. D. Fry, C. Deehr,' and J. Intriligator, From the Sun to the Outer Heliosphere: Modeling and Analyses of the Interplanetary Propagation of the October/November (Halloween) 2003 Solar Events, *J. Geophys. Res.*, 110(A9), A09S10, doi:10.1029/2005JA010939, 2005a.
6. D. S. Intriligator, T. Detman, M. Dryer, C.D. Fry, W. Sun, C. Deehr, and J. Intriligator, Initial comparisons between a 3D MHD approach and the HAFv2 kinematic model: The Halloween 2003 events from the Sun to 6 AU, *The Physics of Collisionless Shocks*, G. Li, G. Zank, C. Russell eds, 304-309, AIP Conference Proceeding 781, 2005b.
7. D. S. Intriligator, T. Detman, W. Sun, C.D. Fry, M. Dryer, C. Deehr, Z. Smith and J. Intriligator, Asymmetries in the Solar Wind from the Sun to 10 AU: Comparison Between a 3D MHD Approach and the 3D HAFv2 kinematic model, in *Proceedings of Solar Wind 11-SOHO*, "Connecting Sun with Heliosphere", Whistler, B.C., Canada, June 13-17, 2005, ESA Publ. Sp-592, pp. 343 - 346, 2005c.
8. D. S. Intriligator, J. Intriligator, W. D. Miller, W. R. Webber, R. B. Decker, W. Sun, T. Detman, M. Dryer, and C. Deehr, Voyager 2 High Energy Ions near the Outward Moving Termination Shock, *Pickup Ions Throughout the Heliosphere and Beyond*, (Eds., J. le Roux, V. Florinski, G. Zank, and A. Coates), Amer. Inst. of Phys. Conf. Proc. 1302, p. 148-157, 2010.
9. D. S. Intriligator, T. Detman, J. Intriligator, C. Gloeckler, W. Sun, W. D. Miller, W. R. Webber,and M. Dryer, Shock Waves in Space Environments, *Shock Waves in Space and Astrophysical Environments*, (Eds., X. Ao, R. Burrows, and G. Zank), Amer. Inst. of Phys. Conf. Proc. 1183, p. 167, 2009.
10. C. N. Arge, and V. J. Pizzo, Improvement in the prediction of solar wind conditions using near-real time solar magnetic field updates., *J. Geophys. Res., 105*, 10,465-10,479, 2000.
11. T. R. Detman, M. Dryer, T. Yeh, S.M. Han, S.T. Wu, and D.J. McComas, A Time-Dependent, 3-D MHD Numerical Study of Interplanetary Magnetic Draping Around Plasmoids in the Solar Wind, J. Geophys. Res., 96, 9531-9540, 1991.
12. S. Han, S. T. Wu, and M. Dryer, A ThreeDimensional, TimeDependent Modeling of SuperSonic, SuperAlfvenic MHD Flow, *Computers and Fluids, 16*, (1), 81103, 1988.
13. L.I. Sedov (1959) Similarity and Dimensional Methods in Mechanics, Gostekhizdat, Moscow, 4th edition, 1957 (English Translation: M. Holt, ed.), Academic Press, New York, 1959.
14. D. S. Intriligator, T. Detman, D. Hamilton, M. Dryer, W. Sun, C. Deehr, and J. Intriligator, Pickup Protons in the Solar Wind: Comparisons of HHMS-PI Simulations and Cassini CHEMS Measurements, *preprint, 2011*.